

Protein Microarray Immobilization via Epoxide Ring-Opening by Thiol, Amine, and Azide

Seyed Mohammad Mahdi Dadfar, Sylwia Sekula-Neuner, Vanessa Trouillet, and Michael Hirtz*

Immobilization of functional molecules in ordered microarrays has vast importance for many applications in sensing and diagnostics. Here, the immobilization of small molecule compounds and protein in microchannel cantilever spotting (μ CS) on epoxy-terminated glass surfaces is studied via ring-opening of epoxides by thiol, amine, and azide, with the purpose of creating microscale patterns for sensing applications. For this, glass surfaces carrying epoxy groups from silanization are functionalized with microarrays by μ CS with different fluorescent and nonfluorescent dyes containing thiol, amine, or azide groups. Experiments with the fluorophores reveal that all routes result in successful immobilization in a short time. Furthermore, from these experiments, optimal reaction conditions including time, temperature, catalyst type, and catalyst amount are determined. The feasibility of these routes in sensing applications is examined by means of protein binding experiments. Comparing the fluorescence intensity values of different biotin carrying spot arrays immobilized on the epoxy-terminated glass surfaces, after incubating the surfaces with fluorescent-labeled streptavidin, reveal the highest surface density of immobilized biotin for the amine route in comparison to the thiol and azide routes. The obtained results from this work can inform the design and fabricating of protein biosensors as well as other biomedical and diagnostic applications.

1. Introduction

Ring-opening of epoxides via nucleophilic attack by thiols, amines, azides, alcohols, cyanides, carboxylic acids, phenols, and hydrazides is of paramount significance in organic synthesis as it provides access to valuable products. Besides the clear significance of these reactions in traditional synthetic arenas and biological/pharmaceutical applications, they are still topic of active research and their future in the preparation of reactive and functional materials appears bright. Generally, in a nucleophilic ring-opening reaction of asymmetric epoxies, depending on reaction conditions, two regio-isomers are possible (Figure 1).^[1–4]

The catalyzed reaction between an epoxy and a thiol, which leads to the formation of a β -hydroxythio-ether linkage, is an efficient, robust, and regio-selective reaction where—if the appropriate kind of catalyst and reaction conditions is employed—high

yield can rapidly achieved. This reaction can be carried out at room temperature and in the presence of air and moisture using a variety of solvents and a few minutes to a few hours is sufficient for completion of the reaction.^[4–6] Formation of reactive hydroxyl groups is a significant aspect of the thiol–epoxy reaction, opening up the opportunity to achieve a second reaction for modification. The polymerization process using monomers carrying thiol and epoxide functionalities can provide well-defined polymers with reactive hydroxyl groups. Subjecting the prepared reactive polymer to a subsequent postpolymerization modification is a valuable route toward the preparation of functional materials.^[7–10] Surface modification via the thiol–epoxy reaction is a useful way for functionalization of different solid substrates. For this, substrates can be designed to carry polymers or immobilized small molecular species containing reactive thiol or epoxide sites. The surface functionalization can then be done either by using another polymer or small molecules with complementary thiol or epoxide groups.^[11–13] The thiol–epoxy reaction has also been extensively used in dual-curable systems with a controlled curing sequence in order to expand adhesives, composites, and high-performance coatings.^[14–21]

β -amino alcohols such as metoprolol, propranolol, atenolol, and dopamine, which are versatile intermediates in the synthesis of various biologically active compounds have earned a valuable place in pharmaceutical and medicinal chemistry.

Dr. S. M. M. Dadfar,^[†] Dr. M. Hirtz
Institute of Nanotechnology (INT) and Karlsruhe Nano Micro Facility (KNMF)
Karlsruhe Institute of Technology (KIT)
Hermann-von-Helmholtz-Platz 1
76344 Eggenstein-Leopoldshafen, Germany
E-mail: michael.hirtz@kit.edu

Dr. S. Sekular-Neuner
n.able GmbH
Hermann-von-Helmholtz-Platz 1
76344 Eggenstein-Leopoldshafen, Germany

V. Trouillet
Institute of Applied Materials (IAM) and Karlsruhe Nano Micro Facility (KNMF)
Karlsruhe Institute of Technology (KIT)
Hermann-von-Helmholtz-Platz 1
76344 Eggenstein-Leopoldshafen, Germany

 The ORCID identification number(s) for the author(s) of this article can be found under <https://doi.org/10.1002/admi.202002117>.

© 2021 The Authors. Advanced Materials Interfaces published by Wiley-VCH GmbH. This is an open access article under the terms of the Creative Commons Attribution License, which permits use, distribution and reproduction in any medium, provided the original work is properly cited.

^[†]Present address: I. Physikalisches Institut (IA), AG Biophysik, RWTH Aachen University, 52074 Aachen, Germany

DOI: 10.1002/admi.202002117

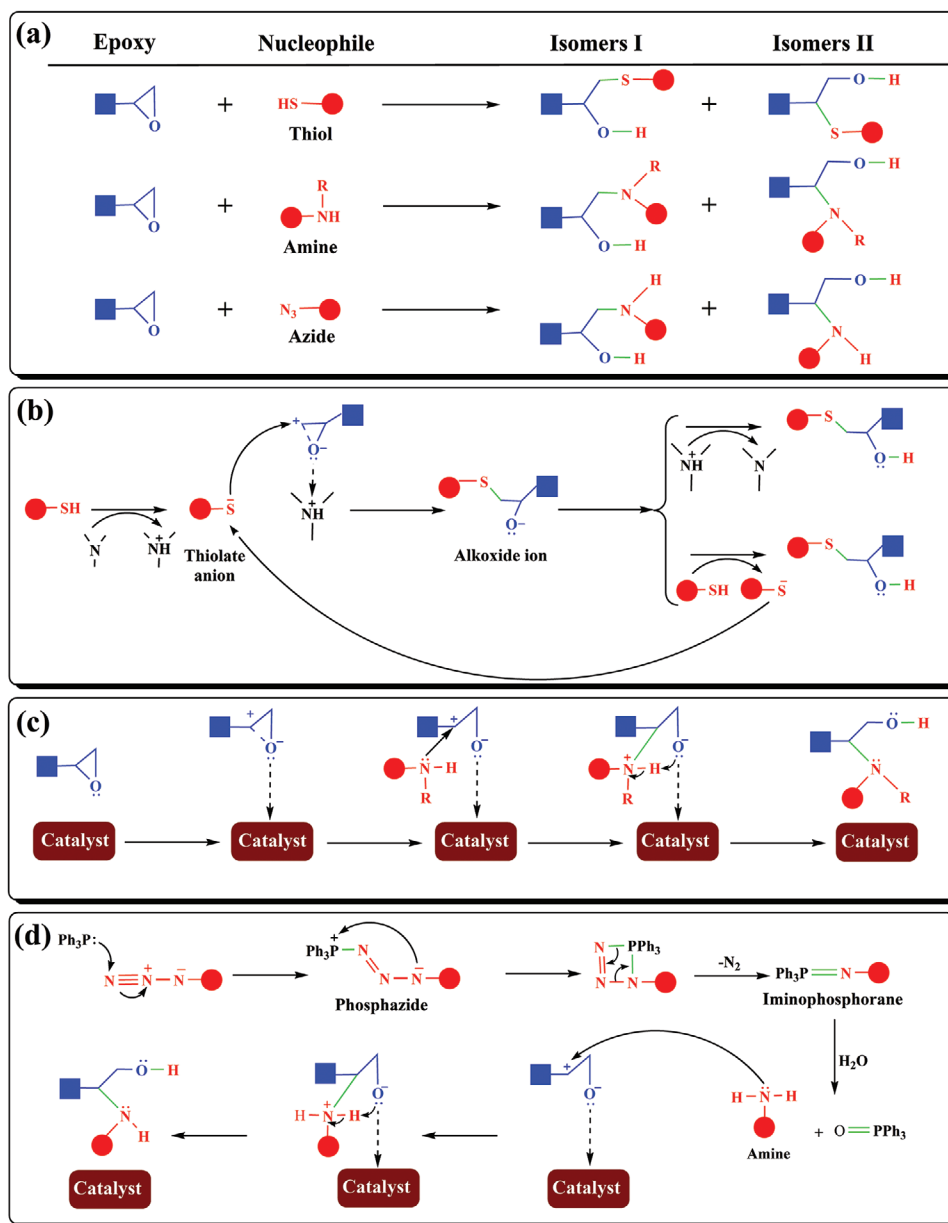


Figure 1. a) The two possible regio-isomers expected from ring-opening reactions of epoxide by thiol, amine, and azide; proposed mechanisms for b) thiol-epoxy reaction initiated by base catalyst, c) amine-epoxy reaction over a heterogeneous catalyst, and d) azide-epoxy reaction via Staudinger reaction.

These materials can be easily achieved via ring-opening of epoxy by a diversified class of amines, but this approach has a slow reaction rate due to the poor nucleophilic character of amine. Therefore, researchers have introduced a variety of homogeneous and heterogeneous catalysts that can enhance the electrophilic character of epoxies. Homogeneous catalytic processes have disadvantages like the use of toxic solvents, the difficulty of separation, and poor reusability of the catalyst. Heterogeneous catalysts also have some limitations like the need for longer reaction times, difficult synthesis of the catalyst, and nonambient reaction conditions.^[22–25]

In contrast to amines and thiols, azides do not directly react with epoxies. Azido groups are greatly suitable for different click reactions or the Staudinger ligation. The Staudinger reaction,

which was discovered by Hermann Staudinger and named after him, is a chemical reaction of an azide with a phosphine or phosphite. This reaction produces an iminophosphorane whose subsequent hydrolysis results in an amine. The produced amine can then react with epoxides via ring-opening.^[26–28]

The design and fabrication of biosensors is of great importance, with implications in innumerable fields. One eminent application case of these sensors is the rapid and accurate detection of proteins (e.g., as cancer biomarkers). For this, molecules that have specific affinity with the protein in question (bioreceptors) should be immobilized on a surface (transducer).^[29–31] In previous works, we prepared microarrays of dyes containing azide or thiol groups on DBCO-terminated glass surfaces^[32] and dyes containing maleimide or DBCO groups on thiol-terminated

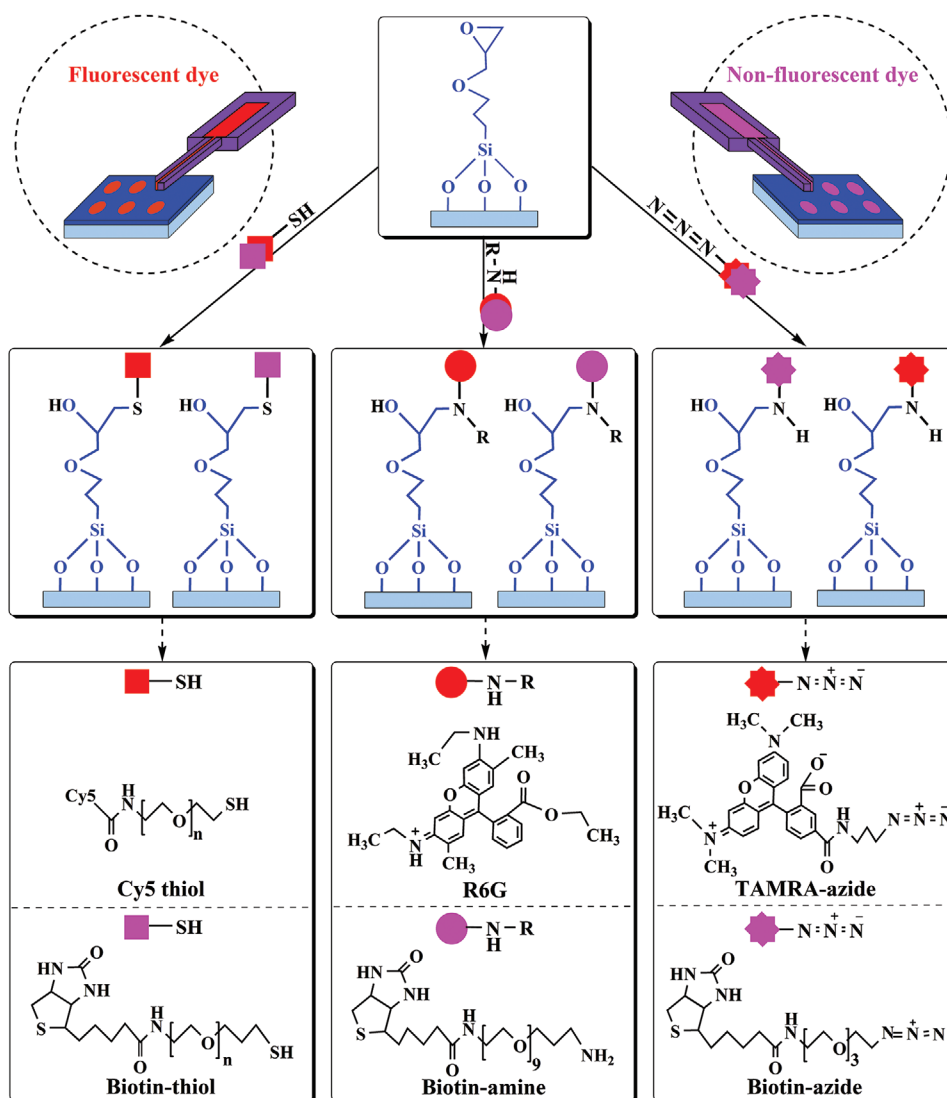


Figure 2. Schematic representation of the chemical immobilization strategies used for functionalization of epoxy-terminated glasses by different fluorescent and nonfluorescent dyes.

glass surfaces^[33] using microchannel cantilevers spotting (μ CS). In order to enable even more flexible choice of immobilization chemistry, in this work, three different routes for the surface functionalization of epoxy-terminated glasses will be examined. Our purpose here is to study the fundamental aspects of thiol–epoxy, amine–epoxy, and azide–epoxy reactions in the context of scanning probe lithography approaches as μ CS, and to document their utilities in the creation of microarrays suitable for sensing applications (Figure 2).

2. Results and Discussion

2.1. Characterization of Surfaces by Contact Angle, Atomic Force Microscopy (AFM), and X-Ray Photoelectron Spectroscopy (XPS)

To obtain epoxy-terminated substrates suitable for the planned immobilization routes, glass substrates were functionalized

with (3-glycidyloxypropyl)trimethoxysilan (GPTMS). Before silanization with GPTMS, the cleaned substrates were subjected to an oxygen plasma treatment to ensure a high density of hydroxyl groups on their surfaces. As a first check of successful functionalization prior to the further experiments, contact angle measurements were done on the hydroxyl- and epoxy-terminated glasses over the course of four weeks. To prevent ink spreading during spotting of microarrays, the water contact angle (WCA) should not be too low. Right after plasma treatment, glass surfaces are highly hydrophilic, with hydrophilicity declining during the course of 3 to 4 weeks, approaching that of a nontreated glass surface again.^[32] The epoxy-terminated surfaces are less hydrophilic, with an initial WCA of $(54.4 \pm 1.5)^\circ$ that stabilizes at around 84.3° (determined by the asymptotic approach of the fit function; Figure 3).

The change in contact angle of the epoxy-terminated surfaces over time might be induced by unmodified hydroxyl groups on the surface decaying until only the thiol groups remain.

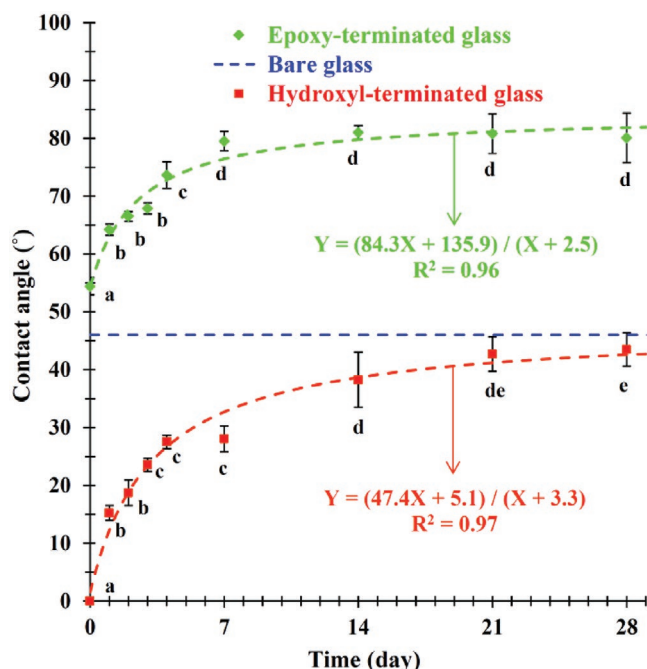


Figure 3. Water contact angles over time on hydroxyl- and epoxy-terminated glasses. Graphs of contact angle over time were fitted by rational function utilizing MATLAB software to give a better guide to the eye. The red and green dashed curves are the best fit for OH-terminated (data taken from ref. [32]) as comparison and epoxy-terminated glass surfaces, respectively. The blue horizontal dashed line represents the contact angle of untreated glass at about 46°. Significant changes in contact angle ($p < 0.05$) are marked by different letters.

Comparing the obtained results for WCA of epoxy-terminated surfaces with those of DBCO-terminated^[32] and thiol-terminated^[33] surfaces studied in previous works reveals the hydrophilicity order as follows: DBCO-terminated surface > thiol-terminated surface > epoxy-terminated surface.

As further measure of surface quality, the roughness of the hydroxyl- and epoxy-terminated glasses as well as of the epoxy-terminated glasses after coating with different fluorescent and nonfluorescent dyes was monitored by AFM (**Figure 4**).

The hydroxyl-terminated glass features a roughness of (0.25 ± 0.02) nm, while the silanization leads to significantly higher roughness $((0.59 \pm 0.16)$ nm). This difference in roughness can be understood due to the possibility of crosslinking between silanes, leading to a less even surface. Further functionalization with Cy5 thiol, TAMRA-azide, biotin-thiol, biotin-amine, and biotin-azide only slightly increases the roughness to (0.62 ± 0.06) nm, (0.60 ± 0.17) nm, (0.64 ± 0.12) nm, (0.64 ± 0.12) nm, and (0.73 ± 0.10) nm, respectively. In contrast, immobilization of R6G on the epoxy-terminated glass leads to significantly higher roughness of (1.35 ± 0.12) nm. This roughness increase could be caused by secondary reactions taking place, as the reaction between R6G (containing a secondary amine) with the epoxy group attached to the surface leads to the production of an active alcohol that can participate in an alcohol-amine reaction.^[34] Therefore, another R6G can add to the surface and the roughness increases. Representative AFM images for the surfaces are given in Figure S1 in the Supporting Information.

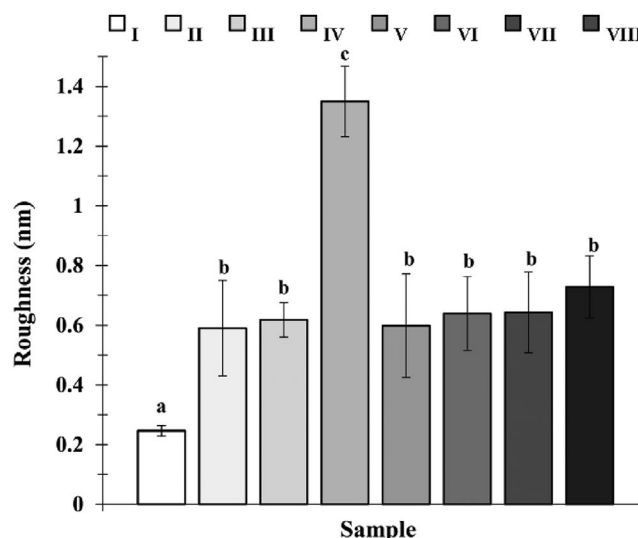


Figure 4. Roughness values as determined by AFM measurements for the I) hydroxyl-terminated and II) epoxy-terminated glass surfaces, as well as for the epoxy-terminated glass surfaces after coating with III) Cy5 thiol, IV) R6G, V) TAMRA-azide, VI) biotin-thiol, VII) biotin-amine, and VIII) biotin-azide, respectively. Significant changes in roughness ($p < 0.05$) are marked by different letters.

In addition to the physical parameters described above, the functionality of the epoxy-terminated substrates was also checked by chemical characterization via XPS, to confirm that the expected chemical reactions are taking place (**Figure 5**).

First of all, the functionalization of the plasma treated glasses with epoxy groups is verified by the main peak observed in the C 1s spectrum at 286.7 eV attributed to C–O^[35] and characteristic here for GPTMS (**Figure 5a**). The attachment of all other molecules can be followed by the appearance of a N 1s signal since all of further immobilized molecules contain some nitrogen in comparison to GPTMS functionalized glasses, for which only a weak nitrogen contamination (0.2 at%) is detected (**Figure 5b–d** bottom). After immobilization of thiol, amine, or azide, a main peak at 400.1 eV can be observed proving essentially the presence of N–C=O and N–CO–N groups present in these various molecules. A further component at 402.2 eV shows in addition the presence of positively charged nitrogen inherent to the attached molecule or in form of hydrogenated amine. Over all, the nitrogen concentration is comprised between 0.8 and 2.5 at%.

2.2. Microarray Immobilization of Cy5 Thiol, R6G, and TAMRA-Azide

To establish the different immobilizations reactions for μ CS and to find optimal reaction parameters, microarrays of fluorescently labeled dyes including Cy5 thiol, R6G, and TAMRA-azide were prepared on the epoxy-terminated glass surfaces using μ CS. After the spotting, ring-opening reactions were allowed to continue for different time durations (10, 20, and 40 min). Furthermore, the reaction between epoxy and Cy5 thiol was examined at room temperature (25 °C) and 37 °C in the presence

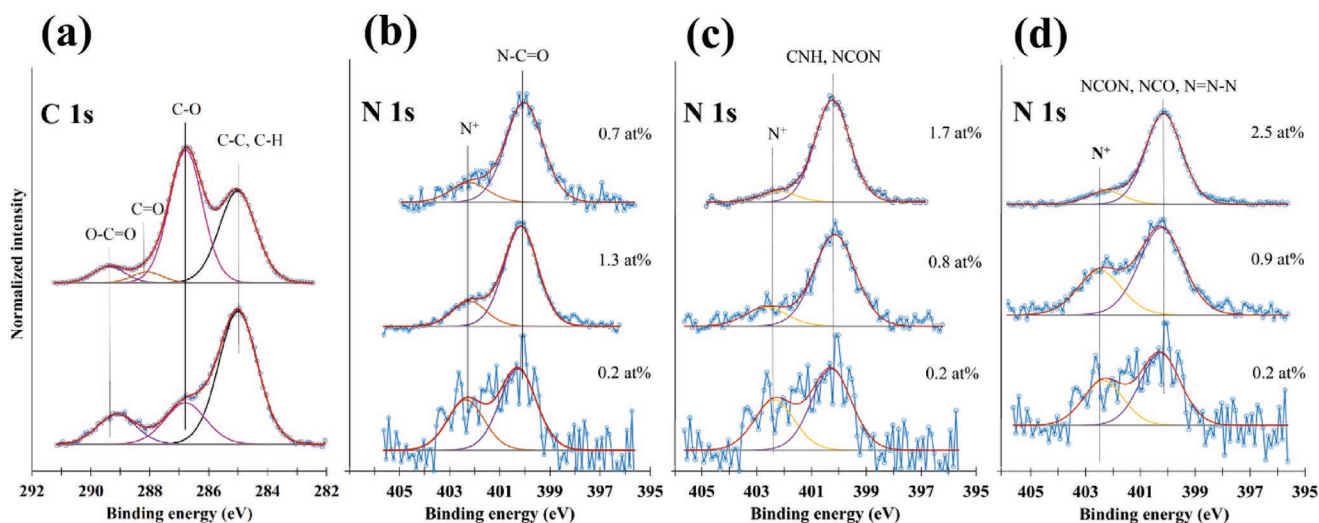


Figure 5. XPS characterization of a) hydroxyl-terminated (bottom) and epoxy-terminated (top) glasses; b) epoxy-terminated (bottom) and epoxy-terminated glass after Cy5 thiol (top) and biotin-thiol (middle) conjugation; c) epoxy-terminated (bottom) and epoxy-terminated glass after R6G (top) and biotin-amine (middle) conjugation and d) epoxy-terminated (bottom) and epoxy-terminated glass after TAMRA-azide (top) and biotin-azide (middle) conjugation. All reactions took place at optimum reaction conditions.

of triethylamine (TEA) as catalyst. Reaction between epoxy and R6G was performed with four different catalysts, at 37 °C and for two different amounts of catalyst (1 and 3 mol%). Bi(OTf)₃, LiCl, Cl₂O₈Zn, and ZnO were used as catalysts to facilitate the reaction between the epoxy and amine groups. For TAMRA-azide, the immobilization on the epoxy-terminated surface was done in a different way: first, the TAMRA-azide was converted into an amine via Staudinger reaction and in the presence of 3 mol% Ph₃P in relation to the azide. Then, the prepared amine ink was mixed with different amounts of Bi(OTf)₃ and spotted on the epoxy-terminated surface. After the reaction time elapsed, the surfaces were rinsed with deionized water, dried by blowing with nitrogen, and were then evaluated by fluorescence microscopy. A summary of results and micrographs of typical lithography outcomes are given in Figure 6.

Obviously, all ring-opening reactions were able to take place in μCS spotting and immobilized the respective fluorophore, as after washing, the patterns remained stable and highly visible in fluorescence. For the epoxy–thiol reaction (Figure 6a), a trend for increased intensity with elevation of temperature and time is visible. However, no significant rise in fluorescence intensity was observed after 40 min (data not shown). Therefore, reaction time of 40 min and reaction temperature of 37 °C is identified as the best conditions for this reaction. The epoxy–amine reaction was studied at 37 °C and for two different amounts of catalyst (Figure 6b–e). Within the screened reaction conditions, by simultaneous consideration of reaction time, catalyst type, and amount, 40 min/3 mol% Bi(OTf)₃, 40 min/1 mol% LiCl, 20 min/3 mol% Cl₂O₈Zn, and 40 min/1 mol% ZnO nanopowder were chosen as the optimal conditions for these reactions, depending on catalyst type, in further experiments. Among different catalysts, Bi(OTf)₃ showed better results than the others in providing clear microarrays with high fluorescence intensity. For reaction between epoxy and azide (which is essentially also an epoxy–amine reaction, as of the ink conversion of the azide via Staudinger reaction), a reaction time of 20 min

and 3 mol% Bi(OTf)₃ were identified as the optimal conditions (Figure 6f). Figure 6g–l show the fluorescence microscope images of micropatterns obtained at the respective optimum reaction conditions.

Although the reaction between epoxy and thiol can take place at elevated temperatures without the need for any catalyst, lower temperatures are feasible by introducing catalysts. Base catalysts such as triethylamine (TEA), diazabicyclo[4.3.0]non-5-ene (DBN), 1,8-diazabicyclo[5.4.0]undec-7-ene (DBU), benzyldimethylamine (BDMA), 1-methylimidazole (1MI), and LiOH are frequently used to catalyze thiol–epoxy reactions. Other catalysts like photobase generators and Lewis acids, which weaken the carbon oxygen bond in epoxide and stabilize the alkoxide ions upon direct attack by the nucleophilic thiol, have also exhibited effectiveness in catalyzing this reaction.^[4,5,36,37] Another important issue for these reactions is the choice of suitable medium. For example, triethylamine in tetrahydrofuran (THF) failed to provide any ring-opening reaction of aliphatic thiols. Interestingly, a change of reaction medium to DMSO could lead to the ring-opening reaction.^[38]

Normally, the reaction between epoxy and amine is performed in the presence of catalysts, although there are some studies^[39,40] for ring-opening of the epoxide groups without catalyst. Ionic liquids, tetrafluoroborate of metals (metal: Li, Zn, Co, Cu, Fe, and Ag), trifluoroacetate of metals (metal: Fe and Ca), perchlorate of metals (metal: Li, Ni, Mg, Co, Zn, and Fe), halides of metals (LiBr, LiCl, AlCl₃, MnCl₂, CoCl₂, BiCl₃, ZnCl₂, and ZnI₂), tungsten salts (WO₂Cl₂, WO₂(acac)₂, and W(OEt₆)), metal oxides in the form of nanoparticles (TiO₂, ZrO₂, Al₂O₃, Fe₂O₃, SiO₂, ZnO, and CuO), triflates of metals ((Bi(OTf)₃, (Zr(OTf)₃, and Cu(OTf)₂), activated heterogeneous mesoporous carbons, sulfated metals (metal: Zr and W), metal amides or triflamides, and biocatalyst are examples of catalysts, which have been successfully employed in aminolysis of various types of epoxy.^[22–24,41–46]

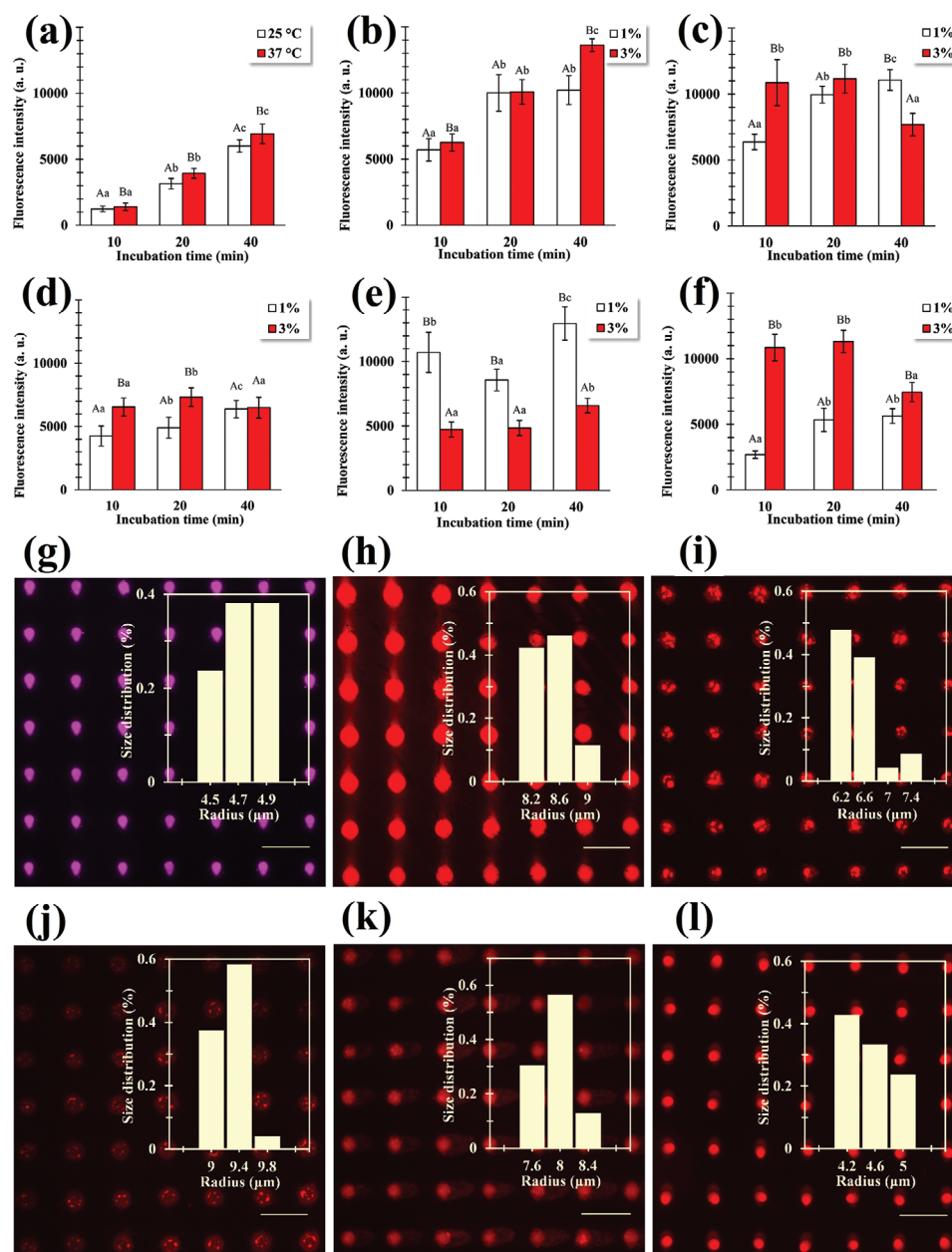


Figure 6. Comparison of results of microarray spotting under different parameters and for selected fluorescent dyes. Obtained fluorescent intensities for a) epoxy–Cy5 thiol at different reaction times and temperatures, and epoxy–RG6 at different reaction times and concentrations of b) Bi(OTf)₃, c) LiCl, d) Cl₂O₈Zn, and e) ZnO, as catalyst, and f) epoxy–TAMRA-azide for different reactions times and concentrations of Bi(OTf)₃ as catalyst. Representative outcomes of spotting at the respective optimal conditions are given for microarrays of g) Cy5 thiol, h) RG6/Bi(OTf)₃, i) RG6/LiCl, j) RG6/Cl₂O₈Zn, k) RG6/ZnO, and l) TAMRA-azide/Bi(OTf)₃, respectively. The scale bars equal 50 μm. The overlay histograms show the distribution of feature radius in the microarrays. For the same reaction time, values with different capital letters and for the same temperature or catalyst concentration, values with different lower case letters are showing a significant difference ($p < 0.05$).

2.3. Protein Coupling by Biotin-Thiol, Biotin-Amine, and Biotin-Azide

In the previous section, we demonstrated successful immobilization of fluorescent Cy5 thiol, R6G, and TAMRA-azide arrays on epoxy-terminated glass through ring-opening reaction. Furthermore, considering the fluorescence intensity values of these microarrays, the optimum reaction conditions were

identified for each of them. However, as different fluorophores used for surface coupling have different functional groups, different emission spectra, and different intensities even for the same surface concentration of immobilized molecules, another strategy should be employed for the direct comparison of these reactions.^[32,33] For this, via epoxide ring-opening routes, biotin-bearing compounds including biotin-thiol, biotin-amine, and biotin-azide were spotted on the epoxy-terminated glasses

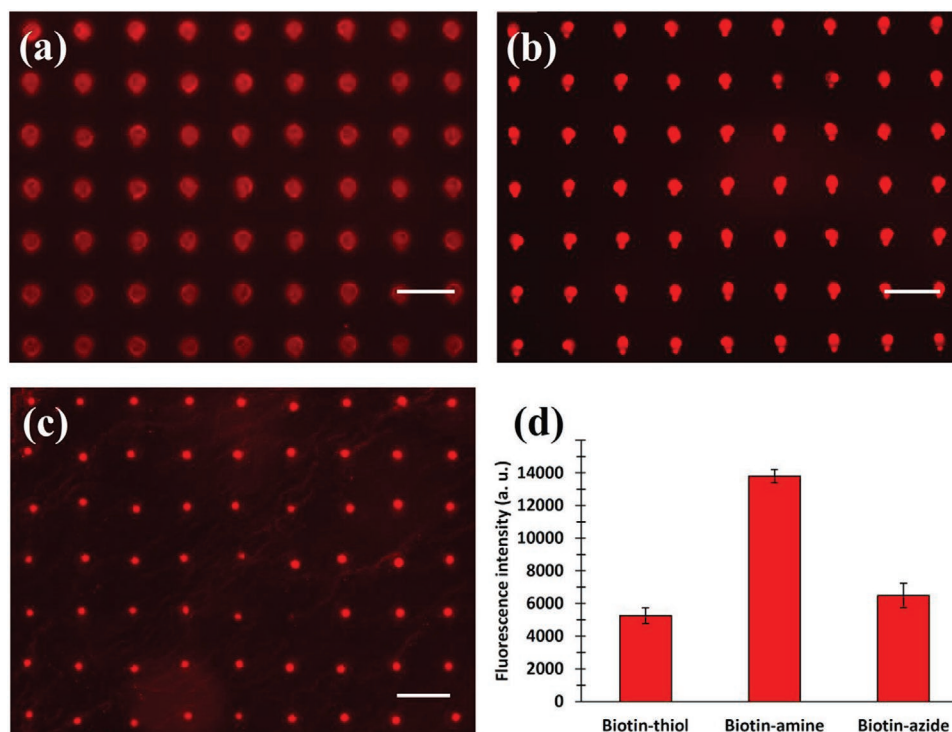


Figure 7. Arrays of a) biotin-thiol, b) biotin-amine, and c) biotin-azide on epoxy-terminated glass after incubating with fluorescently labeled streptavidin (streptavidin-Cy3). The difference in feature size is caused by the different surface tensions of the inks, resulting in more or less spreading of the deposited ink droplet. Scale bars equal 50 μm . d) Chart of obtained fluorescence intensities for the three different immobilization routes.

by μCS into 15×15 spot arrays. Biotin is a frequently used linker having strong affinity with streptavidin.^[47] So, for visualizing the immobilized biotin patterns as well as determination of the amount of immobilized biotin, a fluorescent-labeled streptavidin can be used. Utilizing this technique along with using the same concentrations of a fluorescent-labeled streptavidin can provide a comparison between the different coupling routes. Results for arrays spotted at optimal reaction conditions with the same mole concentrations of biotinylated inks ($2 \mu\text{mol mL}^{-1}$) and fluorescent-labeled streptavidin ($10 \mu\text{g mL}^{-1}$) are summarized in **Figure 7**.

As seen in the representative images, immobilization of the biotinylated compounds for all chemical routes was again successful, as—following incubating the patterns with fluorescent-labeled streptavidin—all become visible under fluorescence microscopy. When comparing the fluorescence intensities of streptavidin bonded on the microarray prepared by these immobilization routes (5257 ± 486) a.u. for the biotin-thiol spots, ($13\,793 \pm 407$) a.u. for the biotin-amine spots, and (6490 ± 742) a.u. for the biotin-azide spots), it is found that ring-opening of epoxy with amine is yielding the highest fluorescence intensity, thus has to be deemed the most effective approach for immobilization of these reactions in μCS .

In previous works, we studied and compared other immobilizing routes including strain-promoted azide–alkyne cycloaddition (SPAAC), thiol–yne coupling (TYC), and thiol–ene Michael addition (TEMA) for the generation of covalently bound microarrays on functionalized glass surfaces, revealing a relative efficiency of reactions as: $\text{TEMA} > \text{TYC} > \text{SPAAC}$.^[32,33] Comparing

the obtained results in the current study with the TEMA route (yielding a fluorescence intensity of (3953 ± 210) a.u. for fluorescently labeled streptavidin)^[33] indicates a more efficient biotin immobilization by the ring-opening of epoxy by thiol, amine, and azide.

3. Conclusion

Our study established the generation of microarrays of small molecules and protein via epoxy ring-opening reaction on epoxy-terminated surfaces. Microarrays of different fluorescent dyes and biotin were created on epoxy-terminated glass via μCS . Different chemical routes over molecules containing thiol, amine, and azide groups were used for immobilization of dyes and inducing the ring-opening reaction on the surface of the epoxy-terminated glass. The ring-opening by fluorescent Cy5 thiol was performed at different temperatures (25 and 37 °C) and times (10, 20, and 40 min) with an optimum found in 37 °C/40 min. R6G was used as fluorescent molecule for amine induced ring-opening of epoxy. As choice and amount of catalyst have important effects on the outcome of amine–epoxy reactions, the effect of four different catalysts ($\text{Bi}(\text{OTf})_3$, LiCl , $\text{Cl}_2\text{O}_8\text{Zn}$, and ZnO nanoparticles) in two different amounts (1 and 3 mol% to dye), at 37 °C was investigated. Screening of different reaction conditions revealed that 3 mol% $\text{Bi}(\text{OTf})_3$ resulted in most efficient immobilization. TAMRA-azide was the third fluorescent molecule used for ring-opening purpose. Here, after the azide was converted into amine via Staudinger

reaction in the presence of 3 mol% Ph₃P, it was spotted with different amounts of Bi(OTf)₃. Here, a reaction time of just 10 min and 1 mol% Bi(OTf)₃ was established as optimal. Finally, comparing the intensities obtained from fluorescently labeled streptavidin as standardized fluorophore on biotin microarrays immobilized under the respective optimal conditions for each route (thiol, amine, and azide), the amine route was found to be the most efficient immobilization strategy. In conclusion, the results of this study recommend the use of an epoxy-amine route to obtain the highest surface density of molecular immobilization.

4. Experimental Section

Materials: Table 1 lists the most important chemicals used in this study. Other chemicals were of analytical grade and were used as received without additional purification steps.

Preparation of Epoxy-Terminated Glasses: Standard glass coverslips (1 cm × 1 cm, VWR, Germany) were subsequently rinsed with chloroform, 2-propanol, and deionized water, and dried under a nitrogen stream. In order to activate the glass surfaces, they were exposed to oxygen plasma (10 sccm O₂, 0.2 mbar, and 100 W, ATTO system, Diener electronics, Germany) for 2 min. The obtained hydroxyl-terminated glasses prepared in this fashion were immersed at room temperature in a 2% (v/v) solution of GPTMS in dry toluene for 5 h. After this time, the epoxy-functionalized glasses were removed from the solution, thoroughly rinsed with acetone, toluene, and deionized water, and dried under a stream of nitrogen.

Ink Solution Preparation: The fluorescent dyes used for the μCS, including Cy5 thiol ($M_w = 3400 \text{ g mol}^{-1}$, $\lambda_{\text{abs}} = 650 \text{ nm}$, and $\lambda_{\text{em}} = 670 \text{ nm}$), R6G ($M_w = 479 \text{ g mol}^{-1}$, $\lambda_{\text{abs}} = 530 \text{ nm}$, and $\lambda_{\text{em}} = 556 \text{ nm}$), and TAMRA-azide ($M_w = 513 \text{ g mol}^{-1}$, $\lambda_{\text{abs}} = 546 \text{ nm}$, and $\lambda_{\text{em}} = 579 \text{ nm}$) were separately dissolved in the mixture of DMSO/glycerol (7:3 v/v) at concentration of 1 μmol mL⁻¹. Also, biotin-thiol ($M_w = 2000 \text{ g mol}^{-1}$), biotin-amine ($M_w = 595 \text{ g mol}^{-1}$), and biotin-azide ($M_w = 445 \text{ g mol}^{-1}$) as nonfluorescent functional compounds were dissolved in a mixture of

DMSO/glycerol (7:3) at a concentration of 2 μmol mL⁻¹ and were used for μCS.

Microarray Printing via μCS: The spotting procedures were performed on a NLP 2000 system (NanoInk, USA) utilizing SPT cantilevers (SPT-S-C10S, Bioforce Nanosciences, USA).^[48,49] Prior to use, the cantilevers were activated by oxygen plasma (10 sccm O₂, 0.2 mbar, 100 W, 2 min) for 2 min. The cantilever reservoirs were filled with 0.2 μL of the respective ink solution. The spotting procedures were implemented at an optimized relative humidity of 20% obtained in previous study.^[32] All patterns were printed with a probe dwell time on the surface of 0.1 s.

Microarray Immobilization: Arrays of fluorescent-labeled dyes including Cy5 thiol, R6G, and TAMRA-azide were spotted onto prepared epoxy-terminated substrates using μCS. After the spotting, the reaction between fluorescent dye and epoxy was allowed to proceed for different time durations (10, 20, and 40 min). Reaction between epoxy and Cy5 thiol was studied at two different temperatures (25 and 37 °C). For a better control of the environmental conditions, the reaction at 37 °C was performed in a temperature chamber (PU-1KP, ESEPC, Japan). Also, for this reaction, 10 mol% TEA was added to the Cy5 thiol ink solution as catalyst. Reaction between epoxy and R6G was performed at 37 °C by adding catalyst into ink solution. Different amounts of four catalysts (Bi(OTf)₃, LiCl, Cl₂O₈Zn, and ZnO nanoparticles) were examined for this reaction. For immobilization of TAMRA-azide on the epoxy-terminated surface, azide was first converted into an amine in the presence of 3 mol% Ph₃P to azide via Staudinger reaction. Then, the prepared amine dissolved in DMSO/glycerol was mixed with different amounts of Bi(OTf)₃ and spotted on the epoxy-terminated surface at 37 °C. After the incubation time elapsed, the samples were washed with deionized water to remove excess ink and stop the reactions and then dried by blowing with nitrogen. For the nonfluorescent dyes (biotin-thiol, biotin-amine, and biotin-azide), the same procedures as fluorescent dyes but with optimum reaction conditions were implemented (Figure 2).

Protein Binding on Biotinylated Microarrays: Arrays of Cy5 thiol, R6G, and TAMRA-azide immobilized on the epoxy-terminated glasses were directly evaluated by fluorescence microscopy. The microarrays of biotin-thiol, biotin-amine, and biotin-azide immobilized on the epoxy-terminated glasses were first incubated with fluorescent-labeled streptavidin in PBS before fluorescence imaging. Prior to adding the streptavidin solution, the microarrays were blocked with 10% BSA in PBS for 30 min. The

Table 1. List of the chemicals used.

Commercial name	Short name	Role	Source
(3-Glycidyloxypropyl)trimethoxysilane	GPTMS	Coupling agent in silanization	Sigma-Aldrich (Germany)
Cy5-labeled polyethylene glycol thiol	Cy5 thiol	Fluorescent dye	Nanocs Company (USA)
Rhodamine 6G	R6G	Fluorescent dye	Sigma-Aldrich (Germany)
5-Carboxytetramethylrhodamine-azide	TAMRA-azide	Fluorescent dye	Jena Bioscience (Germany)
Biotin polyethylene thiol, MW 2000	Biotin-thiol	Nonfluorescent dye (biotinylated molecule)	Nanocs Company (USA)
Biotin-dPEG ₇ -NH ₂	Biotin-amine	Nonfluorescent dye (biotinylated molecule)	Sigma-Aldrich (Germany)
Azide-PEG ₃ -biotin conjugate	Biotin-azide	Nonfluorescent dye (biotinylated molecule)	Jena Bioscience (Germany)
Triethylamine	TEA	Catalyst	Sigma-Aldrich (Germany)
Bismuth(III) trifluoromethanesulfonate or bismuth(III) triflate	Bi(OTf) ₃	Catalyst	Sigma-Aldrich (Germany)
Lithium chloride	LiCl	Catalyst	Sigma-Aldrich (Germany)
Zinc perchlorate	Cl ₂ O ₈ Zn	Catalyst	Sigma-Aldrich (Germany)
Zinc oxide	ZnO	Catalyst	Sigma-Aldrich (Germany)
Streptavidin-Cy3 (fluorescent-labeled streptavidin)	Streptavidin	Conjugation with biotinylated molecules	Sigma-Aldrich (Germany)
Triphenylphosphine	Ph ₃ P	Catalyst	Sigma-Aldrich (Germany)
Dimethyl sulfoxide	DMSO	Solvent	Sigma-Aldrich (Germany)
Bovine serum albumin	BSA	Blocker	Sigma-Aldrich (Germany)
Phosphate buffer saline	PBS	Buffer	Sigma-Aldrich (Germany)

samples were washed by pipetting on and off 30 μL of PBS for three times and then incubated for 1 h with a solution of streptavidin (10 $\mu\text{g mL}^{-1}$, $\lambda_{\text{abs}} = 550 \text{ nm}$, and $\lambda_{\text{em}} = 570 \text{ nm}$) in a dark environment. Last, the samples were washed with PBS and deionized water and blow-dried with nitrogen before inspection by fluorescence microscopy.

Contact Angle Measurements: Static contact angles were measured at room temperature using an OCA-20 contact angle analyzer (DataPhysics Instruments GmbH, Germany). Water droplets of 2 μL were dropped on the surface within 1 s and the average value of contact angle for 5 droplets was measured.

Characterization by XPS: The XPS analysis was performed using a K-Alpha+ XPS spectrometer (ThermoFisher Scientific, East Grinstead, UK) with the Thermo Avantage software for data acquisition and processing. All surface modified surfaces were analyzed using a microfocused, monochromated Al K_{α} X-ray source (400 μm spot size). The spectra were fitted with one or more Voigt profiles (BE uncertainty: $\pm 0.2 \text{ eV}$) and Scofield sensitivity factors were applied for quantification.^[50] All spectra were referenced to the C 1s peak (C–C, C–H) at 285.0 eV binding energy controlled by means of the well-known photoelectron peaks of metallic Cu, Ag, and Au, respectively.

Characterization by AFM: AFM for mapping of roughness was conducted on a Dimension Icon (Bruker, Germany) in tapping mode with HQ:NSC15/Al BS cantilevers (MikroMasch, USA). As a measure for roughness, the root-mean-square (RMS) average of height deviations with regard to the mean image data plane (R_q in the software) was sampled from $5 \times 5 \mu\text{m}^2$ images (4 images per data point) with the AFM system onboard software (NanoScope 3.10, Bruker, Germany). All AFM measurements were done in air and under ambient conditions.

Characterization by Fluorescence Microscopy: The fluorescently-labeled surface patterns were imaged using a Nikon Eclipse 80i upright fluorescence microscope (Nikon, Japan) equipped with an Intensilight illumination (Nikon, Japan), a CoolSNAP HQ2 camera (Photometrics, USA), and a set of Texas Red and Cy5 filters (Y-2E/C, Nikon). Then, average fluorescence intensity per feature was measured with the onboard software (NIS-Elements, Nikon, Japan) by appropriate masking of features and the results were tabulated for the preparation of diagrams and statistical analysis.

Statistical Analysis: The data shown for the different comparisons were expressed in the form of means \pm standard deviations. The significant differences between treatments were analyzed by one-way analysis of variance (ANOVA) and the Duncan tests at $p < 0.05$ using statistical package for the social sciences (SPSS) software version 19.0.0 (Abacus Concepts Inc., Berkeley, California, USA).

Supporting Information

Supporting Information is available from the Wiley Online Library or from the author.

Acknowledgements

This work was partly carried out with the support of the Karlsruhe Nano Micro Facility (KNMF, <https://www.knmf.kit.edu>), a Helmholtz Research Infrastructure at Karlsruhe Institute of Technology (KIT, <https://www.kit.edu>). S.M.M.D. and M.H. gratefully acknowledge support by the Deutsche Forschungsgemeinschaft (DFG) under grant HI 1724/3-1. S.M.M.D. acknowledges support by the German Academic Exchange Service (DAAD) and the Karlsruhe House of Young Scientists (KHYS) in the form of a STIBET grant.

Open access funding enabled and organized by Projekt DEAL.

Conflict of Interest

The authors declare no conflict of interest.

Data Availability Statement

The data that support the findings of this study are available from the corresponding author upon reasonable request.

Keywords

epoxy ring-opening, microarrays, microchannel cantilever spotting, protein immobilization, scanning probe lithography

Received: December 7, 2020

Revised: February 25, 2021

Published online:

- [1] N. Deshpande, A. Parulkar, R. Joshi, B. Diep, A. Kulkarni, N. A. Brunelli, *J. Catal.* **2019**, *370*, 46.
- [2] G. H. Posner, D. Z. Rogers, *J. Am. Chem. Soc.* **1977**, *99*, 8208.
- [3] P. Rani, R. Srivastava, *RSC Adv.* **2015**, *5*, 28270.
- [4] M. C. Stuparu, A. Khan, *J. Polym. Sci., Part A: Polym. Chem.* **2016**, *54*, 3057.
- [5] K. Jin, W. H. Heath, J. M. Torkelson, *Polymer* **2015**, *81*, 70.
- [6] C. E. Hoyle, A. B. Lowe, C. N. Bowman, *Chem. Soc. Rev.* **2010**, *39*, 1355.
- [7] S. De, A. Khan, *Chem. Commun.* **2012**, *48*, 3130.
- [8] S. Binder, I. Gadwal, A. Biemann, A. Khan, *J. Polym. Sci., Part A: Polym. Chem.* **2014**, *52*, 2040.
- [9] I. Gadwal, S. Binder, M. C. Stuparu, A. Khan, *Macromolecules* **2014**, *47*, 5070.
- [10] A. Brändle, A. Khan, *Polym. Chem.* **2012**, *3*, 3224.
- [11] S. B. Rahane, R. M. Hensarling, B. J. Sparks, C. M. Stafford, D. L. Patton, *J. Mater. Chem.* **2012**, *22*, 932.
- [12] R. Iwata, R. Satoh, Y. Iwasaki, K. Akiyoshi, *Colloids Surf., B* **2008**, *62*, 288.
- [13] V. Grazú, O. Abian, C. Mateo, F. Batista-Viera, R. Fernández-Lafuente, J. M. Guisán, *Biomacromolecules* **2003**, *4*, 1495.
- [14] M. Sangermano, M. Cerrone, G. Colucci, I. Roppolo, R. A. Ortiz, *Polym. Int.* **2010**, *59*, 1046.
- [15] C. F. Carlborg, A. Vastesson, Y. Liu, W. van der Wijngaart, M. Johansson, T. Haraldsson, *J. Polym. Sci., Part A: Polym. Chem.* **2014**, *52*, 2604.
- [16] F. Saharil, F. Forsberg, Y. Liu, P. Bettotti, N. Kumar, F. Niklaus, T. Haraldsson, W. van der Wijngaart, K. B. Gylfason, *J. Microchem. Microeng.* **2013**, *23*, 025021.
- [17] D. Guzmán, X. Ramis, X. Fernández-Francos, A. Serra, *RSC Adv.* **2015**, *5*, 101623.
- [18] Y. Jian, Y. He, Y. Sun, H. Yang, W. Yang, J. Nie, *J. Mater. Chem. C* **2013**, *1*, 4481.
- [19] X. Fernández-Francos, A.-O. Konuray, A. Belmonte, S. De la Flor, À. Serra, X. Ramis, *Polym. Chem.* **2016**, *7*, 2280.
- [20] D. Guzmán, X. Ramis, X. Fernández-Francos, A. Serra, *Eur. Polym. J.* **2014**, *50*, 377.
- [21] M. Pepels, I. Pilot, B. Klumperman, H. Goossens, *Polym. Chem.* **2013**, *4*, 4955.
- [22] F. A. Sadique, A. F. Zahoor, S. Faiz, S. A. R. Naqvi, M. Usman, M. Ahmad, *Synth. Commun.* **2016**, *46*, 831.
- [23] E. Ertürk, A. S. Demir, *ARKIVOC* **2008**, *2008*, 160.
- [24] C. Wang, H. Yamamoto, *J. Am. Chem. Soc.* **2014**, *136*, 6888.
- [25] M. Mauri, N. Tran, O. Prieto, T. Hjertberg, C. Müller, *Polymer* **2017**, *111*, 27.
- [26] C. I. Schilling, N. Jung, M. Biskup, U. Schepers, S. Bräse, *Chem. Soc. Rev.* **2011**, *40*, 4840.
- [27] A. Procopio, P. Costanzo, R. Dalpozzo, L. Maiuolo, M. Nardi, M. Oliverio, *Tetrahedron Lett.* **2010**, *51*, 5150.

- [28] T. Meguro, N. Terashima, H. Ito, Y. Koike, I. Kii, S. Yoshida, T. Hosoya, *Chem. Commun.* **2018**, 54, 7904.
- [29] P. Mehrotra, *J. Oral Biol. Craniofacial Res.* **2016**, 6, 153.
- [30] J. Ali, J. Najeeb, M. Asim Ali, M. Farhan Aslam, A. Raza, *J. Biosens. Bioelectron.* **2017**, 8, 235.
- [31] S. M. M. Dadfar, S. Sekula-Neuner, V. Trouillet, H. Liu, R. Kumar, A. K. Powell, M. Hirtz, *Beilstein J. Nanotechnol.* **2019**, 10, 2505.
- [32] S. M. M. Dadfar, S. Sekula-Neuner, U. Bog, V. Trouillet, M. Hirtz, *Small* **2018**, 14, 1800131.
- [33] S. M. M. Dadfar, S. Sekula-Neuner, V. Trouillet, M. Hirtz, *Adv. Mater. Interfaces* **2018**, 5, 1801343.
- [34] J. K. Fink, *Reactive Polymers: Fundamentals and Applications*, Elsevier, New York **2018**.
- [35] S. Hansson, V. Trouillet, T. Tischer, A. S. Goldmann, A. Carlmark, C. Barner-Kowollik, E. Malmström, *Biomacromolecules* **2013**, 14, 64.
- [36] A. O. Konuray, X. Fernández-Francos, X. Ramis, *Polymer* **2017**, 116, 191.
- [37] A. O. Konuray, X. Fernández-Francos, X. Ramis, *Polym. Chem.* **2017**, 8, 5934.
- [38] I. Gadwal, M. C. Stuparu, A. Khan, *Polym. Chem.* **2015**, 6, 1393.
- [39] M. Davydova, A. de los Santos Pereira, M. Bruns, A. Kromka, E. Ukraintsev, M. Hirtz, C. Rodriguez-Emmenegger, *RSC Adv.* **2016**, 6, 57820.
- [40] S. Oberhansl, M. Hirtz, A. Lagunas, R. Eritja, E. Martinez, H. Fuchs, J. Samitier, *Small* **2012**, 8, 541.
- [41] A. K. Chakraborti, S. Rudrawar, A. Kondaskar, *Org. Biomol. Chem.* **2004**, 2, 1277.
- [42] J. S. Yadav, B. V. S. Reddy, A. K. Basak, A. Venkat Narsaiah, *Tetrahedron Lett.* **2003**, 44, 1047.
- [43] T. Ollevier, G. Lavie-Compin, *Tetrahedron Lett.* **2004**, 45, 49.
- [44] A. Kamal, R. Ramu, M. A. Azhar, G. B. R. Khanna, *Tetrahedron Lett.* **2005**, 46, 2675.
- [45] B. Pujala, S. Rana, A. K. Chakraborti, *J. Org. Chem.* **2011**, 76, 8768.
- [46] X. Chen, H. Wu, S. Wang, S. Huang, *Synth. Commun.* **2012**, 42, 2440.
- [47] C. M. Dundas, D. Demonte, S. Park, *Appl. Microbiol. Biotechnol.* **2013**, 97, 9343.
- [48] J. Xu, M. Lynch, S. Nettikadan, C. Mosher, S. Vegasandra, E. Henderson, *Sens. Actuators, B* **2006**, 113, 1034.
- [49] J. Xu, M. Lynch, J. L. Huff, C. Mosher, S. Vengasandra, G. Ding, E. Henderson, *Biomed. Microdevices* **2004**, 6, 117.
- [50] J. H. Scofield, *J. Electron Spectrosc. Relat. Phenom.* **1976**, 8, 129.